Science of the Total Environment 868 (2023) 161639

Contents lists available at ScienceDirect

Science of the Total Environment

journal homepage: www.elsevier.com/locate/scitotenv

Development of human dermal PBPK models for the bisphenols BPA, BPS, BPF, and BPAF with parallel-layered skin compartment: Basing on dermal administration studies in humans

Man Hu [a,b,c], Zhichun Zhang [a,b,c], Yining Zhang [a,b,c], Ming Zhan [c], Weidong Qu [a,b], Gengsheng He [a,b], Ying Zhou [a,b,c,*]

[a] School of Public Health/Centers for Water and Health, Key Laboratory of Public Health Safety, Ministry of Education, Fudan University, Shanghai 200032, China
[b] School of Public Health, Fudan University, Shanghai 200032, China
[c] Pudong New Area Centers for Disease Control and Prevention, Fudan University Pudong Institute of Preventive Medicine, Shanghai 200136, China

HIGHLIGHTS

- Kinetics of BPA alternatives in humans following dermal exposure were investigated.
- Human dermal bioavailability was 26.97 % for BPS in thermal paper.
- Human dermal bio-accessibilities were 31.65 % for BPF and 12.49 % for BPAF in PCPs.
- Parallel-layered skin compartmental model was for the first time applied for BPs.
- Human dermal PBPK models for BPs were developed as useful tools for risk assessment.

GRAPHICAL ABSTRACT

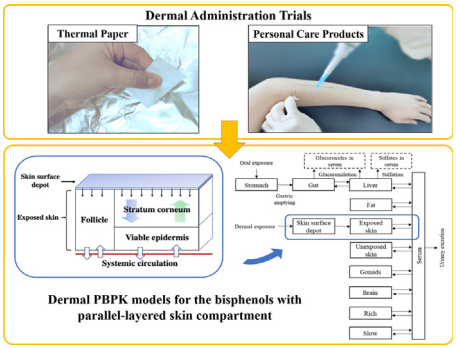

ARTICLE INFO

Editor: Adrian Covaci

Keywords:
Bisphenols
Bio-accessibility
Dermal exposure
PBPK
Human
Risk assessment

ABSTRACT

Risk assessment of human exposure to bisphenols (BPs) including bisphenol A, S, F and AF (BPA, BPS, BPF and BPAF) have suggested that except for ingestion, health risk resulting from dermal contact is not negligible. However, the absorption kinetics of BPA substitutes in humans following dermal exposure have been poorly studied. This study aimed to address the knowledge gap in physiologically based pharmacokinetic (PBPK) modeling of BPA and its high-concerned substitutes (BPS, BPF and BPAF) following dermal administration. Parallel-layered skin compartmental model for dermal absorption of BPs was for the first time proposed and human dermal administration studies were conducted to determine dermal bio-accessibility of BPS from thermal paper (TP) (n = 4), BPF (n = 4) and BPAF (n = 5) from personal care products (PCPs). Further, pharmacokinetics of BPS and its metabolites following human handling TP were investigated and the dermal PBPK models for BPA and BPS were validated using the available human biomonitoring data. Overall, 28.03 % ± 13.76 % of BPS in TP was transferred to fingers followed by absorption of 96.17 % ± 2.78 % of that. The dermal bio-accessibilities of BPs in PCPs were 31.65 % ± 2.90 % for BPF and 12.49 % ± 1.66 % for BPAF. Monte Carlo analysis indicated that 90 % of the predicted variability fell within one order of magnitude, which suggested that the developed PBPK models had medium uncertainty. Global sensitivity analysis revealed that the model uncertainty is mainly attributed to the variabilities of dermal absorption parameters. Compared with the previous models for BPs, the developed dermal PBPK models were capable of more accurate predictions of the internal dose metric in target organs following human dermal exposure to BPs via TP and PCPs routes. These results suggested that the developed human dermal PBPK models would provide an alternative tool for assessing the risk of human exposure to BPs through dermal absorption.

* Corresponding author at: School of Public Health, Fudan University, Shanghai 200032, China.
E-mail address: yingchou@fudan.edu.cn (Y. Zhou).

http://dx.doi.org/10.1016/j.scitotenv.2023.161639
Received 5 October 2022; Received in revised form 19 December 2022; Accepted 12 January 2023
Available online 14 January 2023

1. Introduction

Bisphenols (BPs), including bisphenol A (BPA; 2,2-bis(4-hydroxyphenyl) propane) and its analogues, are a class of chemical compounds containing two phenolic rings linked together by a carbon or sulfonyl group. BPs are the main ingredients of polycarbonate plastics and epoxy resins which have been widely used in the manufacture of packaging materials such as storage containers, drinking bottles, and metal cans (Barboza et al., 2020). The annual global consumption of BPA is approximately 8 million metric tons in 2020 (Chen et al., 2020). Some of BPs are also commonly applied as color developer for the thermal paper (TP) such as cash register receipt, event tickets or self-adhesive labels (Chen et al., 2016; Lehmler et al., 2018). TP has been therefore considered by the European Food Safety Authority (EFSA) as the main source of human exposure to BPA (Eckardt and Simat, 2017). BPs are easily released into the surroundings since they are not chemically bonded to polymeric matrices. At present, BPs have been detected in a variety of environmental compartments like soils (Song et al., 2012), water (Huang et al., 2012; Huang et al., 2020), indoor and air dust (Liu et al., 2019; Zhang et al., 2020), food (Buckley et al., 2019; Liao and Kannan, 2014a), thermal receipt papers (Chen et al., 2016) and personal care products (PCPs) (Lu et al., 2018).

BPA has been considered a typical endocrine-disrupting chemical which showed adverse health effects even at low-dose in both humans and animals, exhibiting potential neurotoxicity, reproductive and developmental toxicity, cardiovascular toxicity (Krishnan et al., 1993; EFSA, 2015), etc. Facing growing restrictions to its use in many countries, some structural analogues of BPA like bisphenol S (BPS), bisphenol F (BPF), and bisphenol AF (BPAF) have been increasingly used for the replacement of BPA. Researchers have found that people are exposed to BPA substitutes worldwide (Liao et al., 2012; Yang et al., 2014; Asimakopoulos et al., 2016; Xue et al., 2015). On the other hand, growing evidences have indicated that BPS, BPF, and BPAF exhibit estrogenic potencies similar to or even greater than BPA through binding to the estrogen receptor (ER) (Chen et al., 2016; Rochester and Bolden, 2015). EFSA recently reported that BPAF showed endocrine activity and adversity based on a systematic review approach considering weight of evidence and mode of action (MoA) (EFSA, 2019). Furthermore, recent in-vitro studies suggested that the conjugated BPS metabolite of BPS-glucuronide (BPS-G) exposure (1 pM–20 μM) disrupted the anti-microbial responses and basal glycolysis human neutrophils (Peillex et al., 2021). Pharmacokinetic data showed that in a French cohort (n = 755) elevated concentrations of BPS-G in human urine were associated with the increased incident of type 2 diabetes (Ranciere et al., 2019). These results indicate that BPS-G cannot be considered as biologically inactive (Rochester and Bolden, 2015). Thus, human exposure to these massively used BPs and their conjugated metabolites have aroused growing public concerns.

An increasing number of monitoring studies and review articles have documented that these high-concerned BPs are ubiquitous in TP and PCPs. In 2019, 187 kt of BPS-based TP were placed on the EU market (EFSA, 2019). A three-year German market analysis showed that BPA and alternatives were frequently used as color developers in TP receipts with the increasing detective frequencies (DF) of from 48.2 % in 2015 to 52.5 % in 2017 for BPA (Eckardt and Simat, 2017). The higher DFs of BPA (77 %) and BPS (72 %) in TP were obtained in China (Yang et al., 2019). Furthermore, the highest DF of BPs in PCPs was obtained for BPAF (38.7 %) followed by BPF (33.3 %) while highest concentrations were detected for BPA (12.8 ng/g) followed by BPF (10.4 ng/g) (Lu et al., 2018). Two previous studies indicated that as much as 27 %–97 % of the unconjugated BPA dose can reach the circulation via human skin exposure (Marquet et al., 2011; Zalko et al., 2011). When both unconjugated and conjugated BPA in the body are considered, dermal contact is the main route of human exposure to BPA (54.12 %) with TP being the dominant contributor (Lu et al., 2018). Recently the amount of BPS transferred from TP to normal skin was found to be higher than the corresponding BPA amount (Karrer et al., 2019). Additionally, dermal exposure to the unconjugated BPs has been proposed to be of equal or even higher toxicological relevance than oral exposure to BPs metabolites (Liu and Martin, 2017; Von Goetz et al., 2017). Therefore, it has been becoming an urgent issue to assess health risks of dermal route of exposure to BPs in humans.

Understanding pharmacokinetics (PK) of BPs following dermal exposure is critical to evaluating human health risks associated with BPs. Physiologically based pharmacokinetic (PBPK) modeling is a valuable tool for quantifying route-specific toxicokinetic behaviors of chemicals. In the previously published human dermal PBPK models for BPs, however, the skin compartment is assumed to be a homogeneous membrane which accordingly ignores the difference resulting from real resistances of human skin layers to absorption of BPs. Several in vitro percutaneous absorption experiments for BPA (Demierre et al., 2012; Toner et al., 2018; Liu and Martin, 2019; Champmartin et al., 2020; Reale et al., 2021), BPS (Liu and Martin, 2019; Champmartin et al., 2020; Reale et al., 2021) and BPF (Lee et al., 2022) have revealed that there exist great differences in dermal absorption PK of BPs. For example, the absorbed dose after 24 h of exposure was 25 % for BPA and 0.4 % for BPS with their respective maximum permeation rates at 670 and 6 ng/cm^2/h (Reale et al., 2021). In addition, the skin absorption parameters for individual BPA substitutes (e.g. the absorption fraction (%) and absorption half-life (h)) were cited from those for BPA (Karrer et al., 2018) in the previous PBPK models for BPs. Consequently, these existing models are not capable of accurate characterizing the in vivo PK of BPA substitutes.

The objective of this study is to address the knowledge gap in physiologically based characterization of dermal PK of high-concerned BPA substitutes. We proposed a human parallel-layered skin compartment model for describing BPs absorption kinetics following dermal exposure. Human dermal administration studies were implemented to determine the dermal bioaccessibility for exposure to BPS from TP as well as for exposure to BPF and BPAF from PCP. PK data from this study and other studies (Sasso et al., 2020; Khmiri et al., 2020) were used for calibration and validation of the developed PBPK models, and Monte Carlo (MC) analysis was conducted for evaluating the uncertainty of the models.

2. Material and methods

2.1. Parallel-layered skin compartment model for BPs

For simulating and modeling of dermal uptake of individual BPs, we proposed a parallel-layered skin compartment model to replace the single homogeneous, well-stirred skin compartment reported by Karrer et al. (2018). As depicted in Fig. 1A, it mainly comprised two layered sub-compartments including the stratum corneum (SC) and the underlying viable epidermis (VE) as well as a parallel "follicle" sub-compartment which represents the shunt pathway of skin appendages (e.g. hair follicles and sweat glands) across the skin. Further, the compartment model assumed that dermal exposure to chemicals would lead to form a skin-surface depot (SSD) where the chemicals might enter the follicle and/or SC sub-compartments. Within the follicle sub-compartment the chemical substances would directly enter the systemic circulation through diffusion, whereas within SC some of them would transfer to the VE sub-compartment through diffusion followed by absorption into systemic circulation, the others would be probably dropped off by desquamation.

The concentration of BPs $\varphi(x,t)$ (nmol/mL) at depth x (cm) and at time t (min) in the SC (Fig. 1) is described by the following equation:

$$\frac{\partial}{\partial t}\varphi(x,t) = D\cdot\frac{\partial^2}{\partial x^2}\varphi(x,t) + u_1\cdot\frac{\partial}{\partial x}\varphi(x,t) \quad (1)$$

where the first term on the right side of Eq. (1) refers to the application of Fick's Second Law, and D (cm^2/min) is the effective diffusivity of BPs through the SC. The second term refers to the process of skin desquamation, in which cells in the SC travel at a velocity of u_1 (cm/min) in a direction opposite to that of BPs.

We further assumed that the concentrations of individual BPs in the SSD ($C_{SSD}(t)$) and the VE ($C_{VE}(t)$) compartments would keep well-stirred at any given time. To obtain solutions to Eq. (1) for values of depth between 0 (the

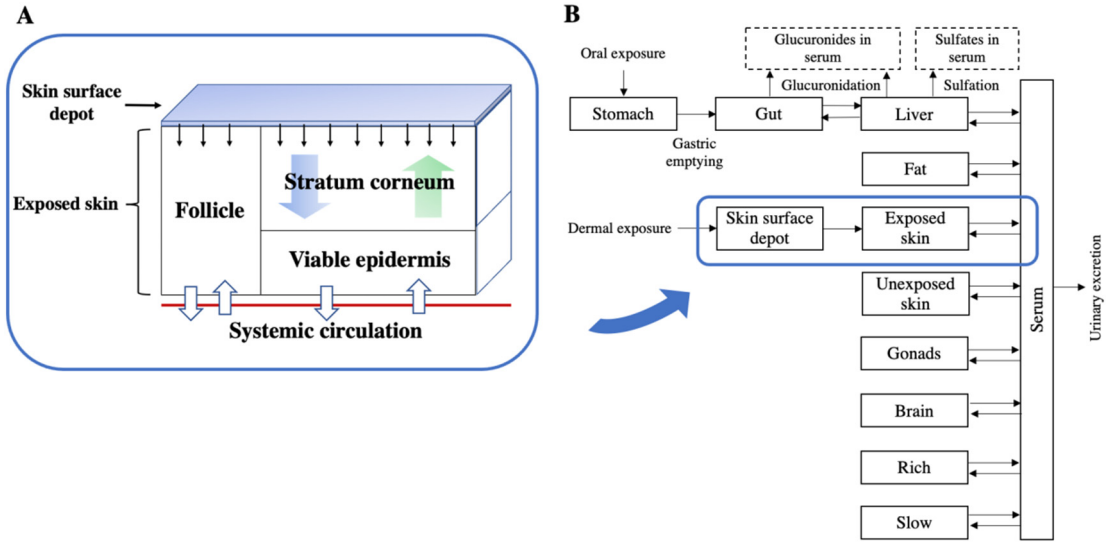

Fig. 1. Schematic diagram of the parallel-layered skin compartment model (A) and the PBPK modeling (B) of human exposure to BPs via peroral and dermal routes. Note: BPs, bisphenols; PBPK, physiologically based pharmacokinetic.

outer surface of the SC and its interface with the SSD) and T_{SC} (the maximum thickness of the SC and its interface with the VE) at times after the initial time t_0, we assumed the concentrations of individual BPs at two boundary conditions would be given by

$$\varphi(0,t) = PCsc \cdot C_{SSD}(t) \tag{2}$$

and

$$\varphi(Tsc,t) = PCscve \cdot Cve(t) \tag{3}$$

where PC_{SC} and PC_{SCVE} are the partition coefficients of two boundary conditions for SC/SSD and SC/VE, respectively. These two boundary conditions reflect instantaneous equilibrium between the SC and SSD at the outer surface of the SC and between the SC and the VE at the interface of those two sub-compartments. An initial condition was given by

$$\varphi(x,t_0) = 0 \tag{4}$$

for all x between 0 and T_{SC}, reflecting an assumption that the SC contained no BPs at the start of skin exposure.

For further numerically solving Eq. (1), we discretized the depth variable x by creating a uniform mesh with 11 nodes ($x_j = T_{SC} \times j \div 10$, for j in 0, 1, …, 10). Then, central finite differences were used to approximate the second-order spatial derivatives in Eq. (1) so that

$$\frac{d}{dt}\varphi_j(t) = D \cdot \frac{\varphi_{j-1}(t) - 2\varphi_j(t) + \varphi_{j+1}(t)}{(T_{sc}/10)^2} + u_1 \cdot \frac{\varphi_{j+1}(t) - \varphi_{j-1}(t)}{2 \cdot (T_{sc}/10)} \tag{5}$$

for j in (1, 2, …, 9) where $\varphi_j(t) \approx \varphi(xj,t)$ and $\varphi_0(t)$ and $\varphi_{10}(t)$ are given by the boundary conditions in Eq. (2) and Eq. (3), respectively.

The flux of individual BPs (nmol/cm^2/min) at a depth x cm into the SC is given by

$$J(x,t) = -D \cdot \frac{\partial}{\partial x}\varphi(x,t) - u_1 \cdot \varphi(x,t) \tag{6}$$

And we used the forward finite difference to compute the value of $J_0(t) \approx J(0,t)$ at the interface of the SSD and the SC as

$$J_0(t) = -D \cdot \frac{\varphi_1(t) - \varphi_0(t)}{(Tsc/10)} - u_1 \cdot \varphi_0(t) \tag{7}$$

The backward finite difference was used to compute the value of $J_{10}(t) \approx J(T_{SC},t)$ as

$$J_{10}(t) = -D \cdot \frac{\varphi_{10}(t) - \varphi_9(t)}{(Tsc/10)} - u_1 \cdot \varphi_{10}(t) \tag{8}$$

The amount of BPs in the VE is given by

$$\frac{d}{dt}A_{ve}(t) = J(T_{SC},t) \cdot E + Q_{VE} \cdot \left(C_B(t) - \frac{C_{VE}(t)}{P_{skin}}\right) \tag{9}$$

where E is the surface area (cm^2) of the SC exposed; Q_{VE} is the blood flow rate (mL/min) into and out of the VE sub-compartment; $C_B(t)$ and $C_{VE}(t)$ are the BPs concentration (nmol/mL) in the arterial blood compartment and VE sub-compartment, separately, and P_{skin} is the partition coefficient for VE/blood.

The amount of BPs in the follicle is given by

$$\frac{d}{dt}A_{FO}(t) = P_{FO} \cdot \left(C_{SSD}(t) - \frac{C_{FO}(t)}{PC_{FO}}\right) \cdot E_{FO} + Q_{FO} \cdot \left(C_B(t) - \frac{C_{FO}(t)}{P_{FO}}\right) \tag{10}$$

where P_{FO} is the permeability coefficient for follicle; PC_{FO} and P_{FO} are the partition coefficients for follicle/SSD and follicle/blood, respectively. E_{FO} is the surface area (cm^2) of the follicle exposed; Q_{FO} is the rate (mL/min) of blood flow into and out of the follicle; and $C_{FO}(t)$ are the BPs concentration (nmol/mL) in follicle.

Therefore, the amount of BPs in the SSD contacting the exposed skin following BPs dermal applied at specific rate (R_{dose}, nmol/min) is given by

$$\frac{d}{dt}A_{SSD}(t) = R_{dose} - J_0(t) \cdot E - P_{FO} \cdot \left(C_{SSD}(t) - \frac{C_{FO}(t)}{PC_{FO}}\right) \cdot E_{FO} \tag{11}$$

2.2. Construction of new dermal PBPK modeling of BPs

In this study, the parallel-layered skin compartment model was introduced into the existing human PBPK model from Karrer et al. (2018). The new dermal PBPK models for BPs (also referred to as adapted model) were developed to improve the prediction accuracy. Specifically, the skin compartment of existing PBPK models for BPs (Karrer et al., 2018) is divided into unexposed and exposed skin compartments (Kapraun et al., 2020; Poet et al., 2000). The former is interconnected with the body via

blood flow (Fig. 1B). The latter is characterized using the parallel-layered skin compartment model (Fig. 1A). The fractional area of the follicle sub-compartment is assumed to be one-hundredth the area of the exposed skin, except for fingertips where no hair follicles exist so that the fraction is assumed to be five-thousandth the area of the exposed skin, and the fractional blood flow to the follicle sub-compartment is assumed to be one fourth the blood flow to the exposed skin (Bookout et al., 1997). The blood flow to VE thus equals to three fourth the blood flow to the exposed skin. The depth of the follicle sub-compartment is assumed to be 388/560 the depth of the exposed skin (Bookout et al., 1997). The blood flow to exposed skin is assumed to be a fraction of the total skin blood flow, which is equal to the fraction of total skin surface area contributed by the application site. The volumes (mL) of the SC, VE and follicle were calculated using skin thickness (cm) and exposure surface area (cm^2) parameters, and the volume of the exposed skin was subtracted from total volume of the skin tissue compartment to get the volume of unexposed skin.

2.3. Parametrization for dermal PBPK modeling of BPs

The bio-accessibility represents the fraction of the total amount of chemical substance in sources, which is exposed to skin surface and available for dermal absorption (Pawar et al., 2017). We introduced parameter F_{TP} to character the fractions of BPS and BPA in TPs transferred to skin, and dermal absorption fractions (F_{absorb}) to describe the maximum absorbed fractions of BPs applied to the exposed skin via TPs or PCPs. Thus, the dermal bio-accessibility of BPA or BPS from TP can be calculated by multiplying the F_{TP} with the corresponding F_{absorb}, while the dermal bio-accessibility of individual BPs from PCPs is equal to the F_{absorb}. In this study we measured the F_{TP} for BPS and F_{absorb} for BPF and BPAF, while the F_{absorb} for dermal exposure to BPA in PCPs was obtained from the experimental study of Biedermann et al. (2010).

Chemical-specific parameters for dermal absorption were calculated by Quantitative structure–activity relationship (QSAR) for dermal penetration compiled from the literature. According to the OECD guidance (OECD, 2007), QSAR should be associated with applicability domain, that is the response and chemical structure space in which the model makes predictions with a given reliability. In the OECD guidance and the current researches on the QSAR models for dermal absorption, the physicochemical parameters of octanol-water partition coefficient ($logK_{ow}$) and molecular weight (MW) were generally used to limit the application domain as we described in Tables S2–S4. Therefore, the QSARs models of which the applicability domain matched with the $logK_{ow}$ and MW of BPs were applied to calculate the permeability coefficient (Kp) in this study. Moreover, for the SC partition and diffusion coefficient, models without such limits were also used for the QSAR calculation. Additionally, the $logK_{ow}$, MW, MV and Mpt for BPA, BPS, BPF, BPAF (Table S1) fell within the applicability domain of these models as shown in Tables S2–S4. In summary, these QSARs comprise: 18 equations for overall skin permeability coefficient (Table S2), 9 for SC/water partition coefficient (Table S3), 7 for SC/VE partition coefficient and 1 for diffusion coefficient (Table S4). All these quantities can be used as input parameters in PBPK models. It's recommended by OECD that the predictivity estimation for the external validation of QSAR model should be conducted by comparing the predicted values with the observed values experimentally tested, which shows the accuracy of the models (OECD, 2007). In the previous in vitro experiments, the Kp value of BPA was reported to range from 1.29×10^{-8} to 1.00×10^{-5} cm/s, which varies with different solvents and exposure concentrations (Champmartin et al., 2020; Demierre et al., 2012; Liu and Martin, 2019). In the present study, the predicted values obtained from 17 QSAR models fell within the range of Kp value mentioned above and thus these models were finally used for the calculation of Kp. Since the Kp value of BPA varied by three orders of magnitude in in vitro studies and was not reported in in vivo studies, we calculated the median value of all 17 predicted results as the initial parameter for Kp in PBPK model, the process of which was also conducted by Gajewska et al. (2014). The comparison of Kp between determined experimentally and predicted with different QSAR models has been presented in Table S2. Besides, since no studies reported the SC partition coefficient and diffusion coefficient for BPs, the median values were also used as the initial parameters. Given that the QSARs are merely available for SC/water partition coefficients, we thus applied the SC/water partition coefficient to SC/SSD partition coefficient in the PBPK models. Due to the current lack of parameters specific to follicle, the overall skin permeability coefficients and SC/water partition coefficient are used for the follicle sub-compartment.

As for other chemical-specific parameters, including tissue-to-serum partition coefficients, the metabolism parameters for the Michaelis-Menten and substrate inhibition enzyme kinetics for glucuronidation and sulfation, and physiological parameters like urinary excretion rate, we applied the same values as reported by Karrer et al. (2018).

2.4. Dermal bio-accessibility of BPS, BPF, and BPAF

The human volunteer study was performed for determining F_{TP} of BPS and F_{absorb} of BPs. The study protocol was approved by the Institutional Review Board (IRB) of the School of Public Health, Fudan University (IRB00002408&FWA00002399) (approval number: IRB#2020-12-0865) and informed consent was obtained from all subjects before participating in this study. Eight healthy volunteers (4 males and 4 non-pregnant females, ages 21 to 47, weights 43.6 to 76 kg, all Chinese) who did not suffer from chronic illness were recruited. None of the volunteers used any medications during the study period and reported occupational exposure to BPs. See the supplementary information (SI) for more details. The volunteer study was described as follows.

Four volunteers (2 males and 2 females) participated in the dermal administration study in which BPS was dermally administered to each volunteer through handling TP (0.1 g/piece) containing a deuterated BPS (BPS-d_8) dose of 1.0 mg/g TP, corresponding to the average concentration of BPS detected in seven categories of TPs purchased from Chinese markets (Yang et al., 2019). The study procedure was represented in Fig. 2A. Briefly, the individual volunteer was firstly asked to sample both hands with water moistened Kimwipes for checking any background exposure; after letting hands dry naturally, each volunteer was dermally administered at a fixed dose of BPS-d_8 by repeatedly handling a piece of TP together with their thumb, forefinger and middle finger for exact 10 min (t1) corresponding to the average time of individuals handling receipts reported by Bernier and Vandenberg (2017), and all applied TP samples were recycled for testing the residuals of BPS-d_8; volunteers then put nitrile gloves on both hands to avoid contamination from environment, which lasted a series of dermal administration periods (t2) including 10 min, 30 min, 60 min and 120 min, respectively; after that, the nitrile glove was removed and collected for further testing and the administrated fingers were washed with ethanol (80 mL/hand) for 2 min and the washing solvent was also collected for testing residuals of BPS-d_8 on fingers; finally, volunteers cleaned their hands with warm water and soap.

Four volunteers (1 male and 3 females) participated in the dermal application study for BPF and so did five volunteers (2 males and 3 females) for BPAF. The fixed dose of BPF-d_{10} or BPAF-$^{13}C_{12}$ was pipetted into the vehicle of simulated PCPs which consisted of glycerin (99.5 % purity) and sodium carboxymethylcellulose (10 mg/mL) followed by 1:1 (v/v) dilution with ultrapure water. As for the dermal administration study of BPF, the simulated PCPs sample at a dose of 0.117 ng/cm^2 for BPF-d_{10} was dermally applied on a marked rectangular surface of 60 cm^2 for each forearm of the individual volunteer over a series of administration periods including 0 min, 240 min, 360 min, 480 min, 720 min, 840 min, 960 min, 1080 min and 1200 min, respectively; as for the dermal administration study of BPAF, the individual volunteer was exposed to the simulated PCPs vehicle sample at a dose of 0.083 ng/cm^2 for BPAF-$^{13}C_{12}$ over a series of administration periods including 0 min, 5 min, 10 min, 15 min, 25 min, 30 min, 45 min, 60 min and 360 min, respectively. Overall, the individual volunteers were dermally applied to 14.04 ng of BPF-d_{10} or 9.96 ng of BPAF-$^{13}C_{12}$, which were comparable with the estimated daily dermal exposure levels of BPs in female adults (Liao and Kannan, 2014b). As shown in Fig. 2B, the forearms of volunteers were firstly sampled by ultrapure water-

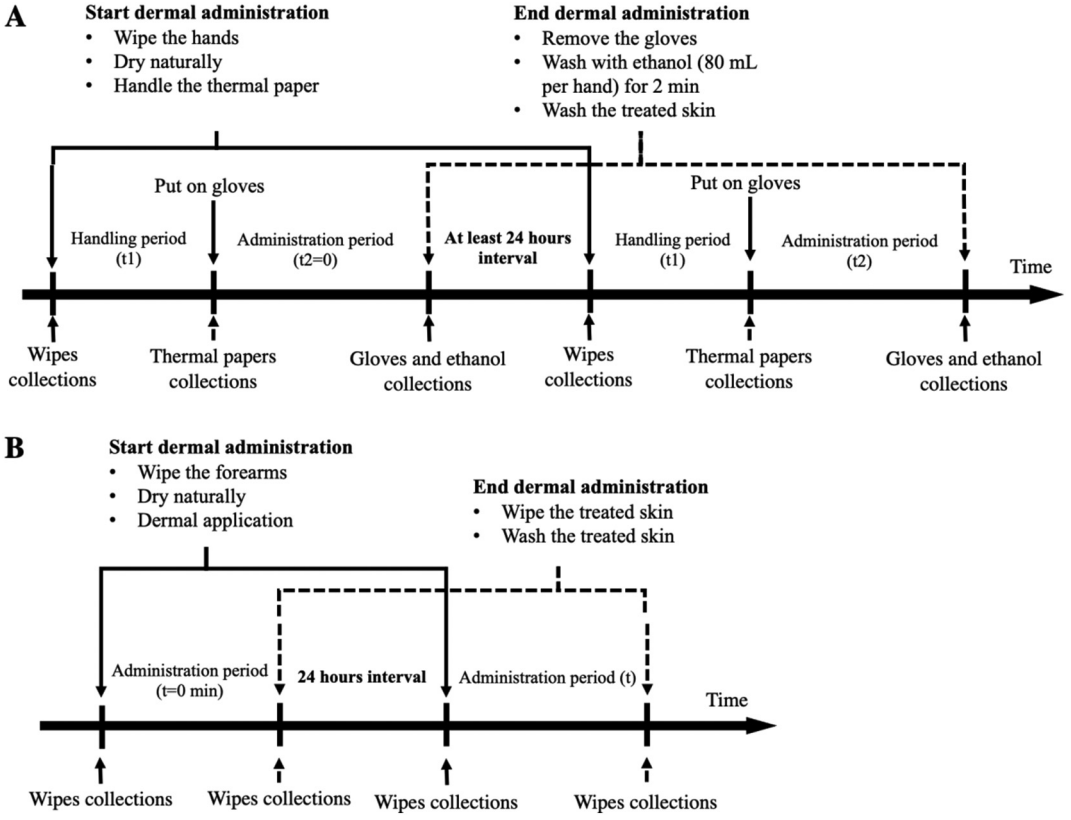

Fig. 2. The process flow charts of the dermal administration studies for BPS (A) and BPF, BPAF (B); Note: BPS, bisphenol S; BPF, bisphenol F; BPAF bisphenol AF.

moistened Kimwipes, and then the designated skin area was administrated with the simulated PCPs sample and kept untouched by ambient environment until the end of the administration period; after that, the wetted wipes were used to clean the treated area; all the collected samples were stored at −20 °C for analysis. Sample treatment and analysis of BPS, BPF and BPAF would be provided in the SI.

The study for BPS, BPF and BPAF were conducted independently without time overlapping and the intervals between each dermal administration of BPs were set no <24 h to avoid interference as far as possible.

Based on the dermal administration study mentioned above, F_{TP} and F_{absorb_BPS} for BPS were calculated as follows,

$$F_{TP} = \frac{M_{TP0} - M_{TP1\_t1}}{M_{TP0}} \times 100\% \quad (12)$$

$$F_{absorb\_BPS} = \max\left(\frac{M_{TP0} - M_{TP1_{t1}} - M_{gloves_{t2}} - M_{ethanol_{t2}}}{M_{TP0} - M_{TP1_{t1}}}\right) \times 100\% \quad (13)$$

Here, M_{TP0} and M_{TP1_t1} refer to the amounts of BPS-d_8 in TPs before and after handling, respectively. M_{gloves_t2} and $M_{ethanol\_t2}$ refer to the residual amounts of BPS-d_8 on gloves and on exposed fingers extracted by ethanol at administration period t2.

$F_{absorb\_BPF/BPAF}$ for BPF or BPAF were calculated as follows,

$$F_{absorb\_BPF/BPAF} = \max\left(\frac{M_{PCP} - M_{wipes_t}}{M_{PCP}} + \frac{M_{PCP} - M_{wipes_{t=0}}}{M_{PCP}}\right) \times 100\% \quad (14)$$

Here, M_{PCP} refers to the amount of BPF-d_{10} or BPAF-$^{13}C_{12}$ in the simulated PCPs. M_{wipes_t} and $M_{wipes\_t=0}$ refer to the residual amount of BPF-d_{10} or BPAF-$^{13}C_{12}$ on the exposed forearm at administration period t and at zero. The $M_{wipes\_t=0}$ was introduced for correction of the baseline of wipes extract efficiency.

2.5. Calibration and adjustments of PBPK models

To further investigate the pharmacokinetics of BPS in human body following dermal exposure to BPS via handling TP, we implemented a dermal administration study. The study protocol was also approved by the Institutional Review Board (IRB) of the School of Public Health, Fudan University (IRB00002408&FWA00002399) (approval number: IRB#2020-12-0865) and informed consent was obtained from all subjects before participating in this study. This study was conducted one month later to avoid the interference from the previous dermal administration studies (Khmiri et al., 2020). A dose of 10 mg/g for BPS-d_8 was applied to four individual volunteers (3 males and 1 female) for assessing measurable levels of unconjugated BPS-d_8 and total BPS-d_8 (the sum of unconjugated BPS-d_8 and BPS-d_8 glucuronide (BPS-g-d_8)) (Khmiri et al., 2020; Oh et al., 2018) in urine. The similar procedure as shown in Fig. 2A was carried out for t1 at 10 min and t2 at 120 min, besides the additional urine sampling. In brief, the last urinating prior to this trial was collected to test the background level of each volunteer exposure to BPS-d_8. Volunteers were asked to collect 72-h urine samples and record every micturition time. Meanwhile the urine volumes were immediately measured using clean graduated cylinders. Following each sampling 10 mL of urine sample was prepared in 15 mL polypropylene tubes and stored frozen at −20 °C until analysis. Sample analysis of total and unconjugated BPS-d_8 in urine specimen was provided in SI.

We found that the ratio of unconjugated BPS to BPS-g in terms of urine excreted amount predicted by the previous PBPK model from Karrer et al. (2018) was inconsistent with the observed data (Oh et al., 2018) and speculated that this discrepancy might result from the previous PBPK model calibration depending solely on serum kinetics data whereas neglecting urine kinetics. Therefore, we firstly recalibrated the previous oral PBPK model for BPS based on both measured serum and urine data from Oh et al. (2018) to adjust the model parameters to fit with volunteer in this study, which has different individual physiological parameters and BW-specific single per-oral exposures from the those of the previous model (Karrer et al., 2018). The R function “optim” was used to minimize the sum of squared error

(SSE) between the estimated and observed data. Then, the adapted PBPK model for dermal exposure to BPS was calibrated by comparing the model predictions based on individual volunteer physiological parameters and the measured dermal exposure levels with the time-course urine excretion amount of unconjugated BPS and the total BPS derived from the sum of unconjugated BPS and BPS glucuronide (BPS-g) obtained in this study. Subsequently, we adjusted the model to get a good correlation with the biomonitoring data using R function "optim" to minimize the sum of squared error (SSE) between the predictions and kinetics observed experimentally. The biomonitoring volunteer data used for model calibration can be open access in the Github data depository: https://github.com/YingZhou8/PBK.git.

2.6. Validation of the PBPK models for BPA and BPS

The validation dataset should be independent of the dataset for model calibration. In the present study, the adapted PBPK model for BPA and the calibrated PBPK model for BPS was validated using the dataset obtained from Sasso et al. (2020) and Khmiri et al. (2020) respectively. Sasso et al. (2020) dermally administrated deuterated BPA (BPA-d_6) to ten healthy volunteers and collected the blood and urine samples over 144 h after treatment for separate analysis of the total and unconjugated BPA-d_6. Khmiri et al. (2020) orally and dermally administrated BPS to eight healthy volunteers. Blood samples were collected over 48 h after treatment and complete urine voids pre-exposure and over 72 h postdosing. BPS-d_8 and BPS-g-d_8 were tested separately. In this study, the average volunteers' physiological parameters were used for the validation of our PBPK models. The F_{absorb} for BPS dermal via simulated PCPs was set at 23.4 % which equals to the sum of average recoveries of BPS in skin tissue (17 %) and receiver solution (6.4 %) at high dose of in vitro skin permeability experiments (Liu and Martin, 2019).

We did not carry out the calibration and validation of PBPK model for BPF and BPAF in this study, since kinetics data in human body for BPF and BPAF were currently unavailable.

2.7. Sensitive analysis and uncertainty analysis

Local sensitivity analysis commonly does not investigate the impact of parameters correlations on model outputs since it generally does not consider parameters having a specific distribution. Global sensitivity analysis (GSA) which samples all parameters over their specific distributions, however, can evaluate simultaneously the relative contributions of all model parameters and their potential interactions to a set of specified model outputs variance (Li et al., 2010). Therefore, GSA was conducted with the "soboljansen" package of R language used for assessing the model parameters importance while considering their uncertainty and correlations in this study. Maximum concentration (C_{max}) and 24-h area under the curve (AUC) of unconjugated BPS in human blood were considered as model outputs.

Monte Carlo (MC) simulation was used to assess the uncertainty on the model output. In the MC analysis, values are randomly sampled from probability distributions defined for variables of interest. As for F_{TP} and F_{absorb} measured in this study, truncated normal distribution was used to account for uncertainty in a physiologically plausible way (95 % of the distributions equals measured mean ± 1.96 times standard deviation (SD)). As for F_{absorb} of BPA for PCPs exposure pathway and chemical-specific parameters for dermal absorption, we randomly varied the parameters using truncated normal distributions. Among them, the mean values were derived from parametrization of our adapted models and coefficients of variation (CV = SD / mean) were used to describe the relative extent of variability at the value of 30 %.

Other model parameters, including physiological (Table S5) and chemical-specific parameters (Tables S6–S9), were randomly sampled under either truncated normal distribution or trapezoidal distribution adopted from Karrer et al. (2018). We conducted the uncertainty analysis for serum concentrations of BPs in women of childbearing age (18 to 45 years). 4 μg/kg bw/day was used via both the dermal exposure pathways as model inputs for all BPs (EFSA, 2015). We simulated dermal exposure by touching TP and using PCPs twice a day, in the morning and in the evening corresponding with Karrer et al. (2018, 2019). The simulation was run for 4 d to achieve a steady-state concentration in serum. Each MC simulation included 10,000 iterations. Uncertainty coefficients which equal the ratio of 95th percentile (P95) and median (P50) of the model outputs were used for evaluating model uncertainty and the values greater than or equal to 2, between 0.3 and 2 and less than or equal to 0.3 correspond to high, medium and low uncertainty, respectively (WHO, 2010).

2.8. Model application

The adapted models were utilized to predict the toxicokinetic process of four BPs when adult women (18 to 45 years) are exposed to them via TPs and/or PCPs routes. The concentrations of unconjugated BPs in gonads of female adults were applied to outcome metrics since the gonads are susceptible to the effects of exposure to endocrine disrupting chemicals (Karrer et al., 2018). The dermal exposure scenario used for uncertainty analysis was also applied for the evaluation. PBPK models were run for 4 days to yield the stable concentration–time curve of individual BPs in gonads. The predictions of the adapted dermal PBPK models were also compared with those of the previous ones (Karrer et al., 2018).

2.9. Computing software

All model simulations were run in DeSolve using R software (version 4.0.1, 2020; R Development Core Team, http://www.R-project.org). The model code can be open access in the Github data depository: https://github.com/YingZhou8/PBK.git.

3. Results

3.1. Model parametrization and calibration for BPs

The measured F_{TP} for BPS exposure via handling TP was 28.03 % ± 13.76 % (Fig. 3A) and the corresponding F_{absorb} values at different dermal administration periods were not significantly different (Wilcoxon test, $p > 0.05$) with an average of 96.17 % ± 2.78 % (Fig. 3B), thereby resulting in the average dermal bio-accessibility of 26.96 % for BPS in TPs. The obtained dermal bio-accessibility of BPS was also applied to BPA model via TP exposure pathway in this study. The F_{absorb} through PCPs exposure were 31.65 % ± 2.90 % for BPF (Fig. 3C) and 12.49 % ± 1.66 % for BPAF (Fig. 3D), respectively. The values of other chemical-specific parameters describing dermal absorption process in PBPK models for targeted BPs were summarized in Table 1.

As for the previously reported PBPK model for BPS, Karrer et al. (2018) merely applied serum-related biomonitoring data to calibrate the urinary excretion parameters for BPS exposure. We therefore found that the predicted amounts for unconjugated BPS in urine using the previous PBPK model (Karrer et al., 2018) were apparently higher than the measured urinary data from a study on the PK of BPS in adults (Oh et al., 2018) (Fig. S1c). However, when we adjusted the model parameters with a decrease of the urinary excretion for unconjugated BPS (from 0.30 to 0.04 L/h/kg $BW^{0.75}$) and a moderate increase of the urinary excretion for BPS-g (from 1.20 to 1.34 L/h/kg $BW^{0.75}$), as shown in Fig. S1(e–h), the model predictions were considerably improved after calibration of the BPS model. Consequently, in the present study the adjusted urinary excretion parameters for unconjugated BPS and BPS-g was applied to our PBPK model for BPS.

The urinary PK of BPS in four volunteers following fingers exposure to the dosing TPs dosing of 10 mg BPS-d_8/g paper was investigated to calibrate the proposed dermal PBPK model for BPS in the study. As shown in Fig. S2, prior to exposure to the contaminated TPs, BPS-d_8 and its metabolites were not detectable in urine from all volunteers. Over post-exposure 2–3 d, the total and unconjugated BPS-d_8 were detectable in 76.4 % and 27.3 % of urine samples (n = 55) from all participants, respectively. The

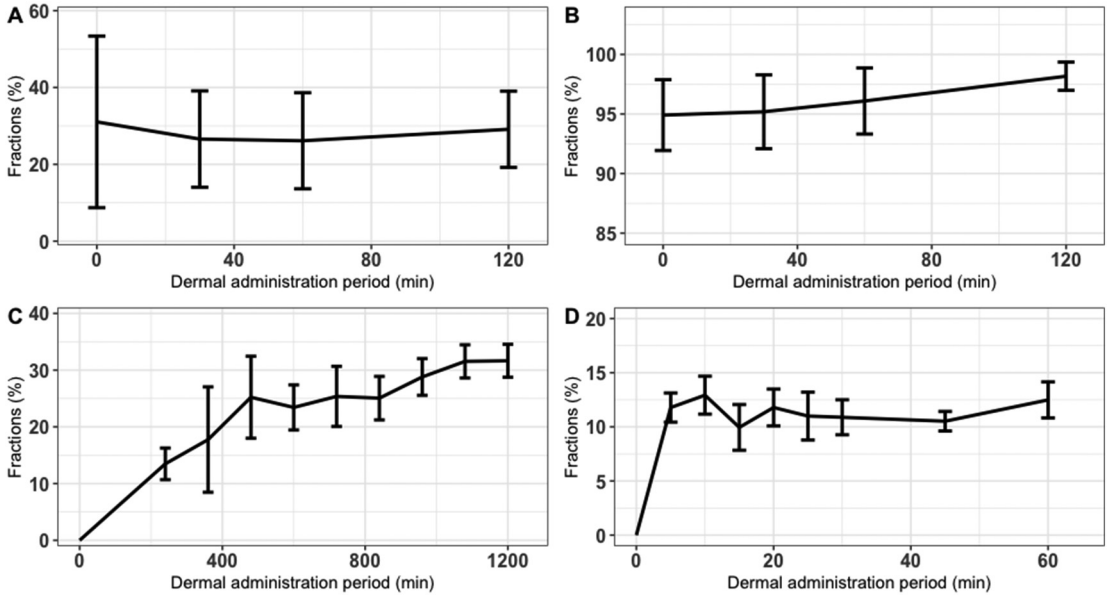

Fig. 3. The time course plots of fraction for BPS transferred to fingers via handling TP (A) and its dermal absorption fractions (B) and dermal absorption fractions for BPF-D_{10} (C) and BPAF-$^{13}C_{12}$ (D) via dermally administrated the simulated PCPs. Note: BPS, bisphenol S; BPF, bisphenol F; BPAF bisphenol AF; PCPs, personal care products.

proportion of urinary unconjugated BPS-d_8 to total BPS-d_8 was 11.10 % ± 3.79 %. The detectable urinary levels of total BPS-d_8 were observed on average at 5.75 h after the start of dosing. The urinary maximum concentration (C_{max}) of total BPS-d_8 occurred at 14 to 29 h and ranged from 0.036 to 0.17 ng/mL (Fig. S2). In summary, the cumulative urinary excretion of total BPS-d_8 accounted for 0.002 % of the applied dose in TPs and 0.012 % of the actual absorbed dose.

As shown in Fig. 4, the observed cumulative excretion amounts of total BPS and unconjugated BPS in urine at first rose rapidly and then rose slowly until they reached a plateau. Prior to model calibration, the simulated cumulative excretion of total BPS and unconjugated BPS in urine presented higher amounts compared with the observed biomonitoring data from this study (Fig. 4a–b). As for the model from Karrer et al. (2018), the predicted cumulative excretion of total and unconjugated BPS in urine also presented higher amounts compared with the observed biomonitoring data (Fig. S9). After adjusting the model parameters with the increases of the D, P_{FO} and u_1 (Table 1), however, a good consistency between the observed and simulated data was obtained (Fig. 4c–d). These calibrated parameters of urinary excretion for BPS model were also applied to BPAF model in this study.

3.2. Model validation for BPA and BPS

As for validation of BPA model, the pharmacokinetic parameters for human dermal exposure to BPA predicted by the dermal PBPK model for BPA adapted in this study were compared with those derived from human dermal administration study (Sasso et al., 2020). As shown in Table 2, the predicted mean values of C_{max} and AUC for unconjugated BPA-d_6 in serum were 0.74 and 0.98 times of the observed values, respectively, and the predictions of those for total BPA-d_6 in serum were 0.87 and 0.94 times of the observed values. In addition, the predicted urine cumulative excretion of total BPA-d_6 was 1.31 times the measured values.

The calibrated dermal PBPK model for BPS was also validated using toxicokinetic data from Khmiri et al. (2020). For preoral exposure, the predicted mean values of C_{max}, AUC and urinary cumulative excretion were 0.73, 1.03 and 0.92 times of the measured values for unconjugated BPS-d_8 and 0.52, 0.55 and 1.03 times of the measured values for BPS-g-d_8, respectively (Table S11). In comparison with the measured biomonitoring data, the predicted average values for serum concentrations of BPS-g (Fig. 5B), except for serum concentrations of BPS (Fig. 5A) seemed to be moderately lower. However, urine excretion of BPS (Fig. 5C) and BPS-g (Fig. 5D) fell within one standard deviation of the mean from an estimation of individual measurements. In addition, the serum concentration and urine cumulative excretion amount of unconjugated BPS and BPS-g following dermal exposure via PCPs route simulated by Karrer et al. model was quite far from the experimental data from volunteer study (Fig. S10). These results suggested that the predictability of the adapted model for the serum concentration and urine cumulative excretion of human exposure to BPs via PCPs route has been obviously improved.

Table 1
Chemical specific parameters for dermal absorption in PBPK models for BPA, BPS, BPF, and BPAF.

Chemical specific parameters	Symbol	BPA	BPS	BPF	BPAF
Follicle permeability coefficient ($\times 10^{-4}$)	P_{FO}	10.55	0.64	12.68	7.42
SC diffusion coefficient ($\times 10^{-10}$)	D	2.34	1.73	0.50	0.076
SC desquamation velocity ($\times 10^{-5}$)	u1	5.70	5.70	5.70	5.70
SC/water partition coefficient	PC_{SC}	64.60	5.40	42.40	142.30
SC/VE partition coefficient	PC_{SCVE}	195.12	19.45	137.60	265.30
VE/blood partition coefficient	Pskin	2.15	0.92	1.09	3.26

Note: PBPK, physiologically based pharmacokinetic; BPA, bisphenol A; BPS, bisphenol S; BPF, bisphenol F; BPAF bisphenol AF; SC, stratum corneum; VE, viable epidermis.

3.3. Sensitive analysis and uncertainty analysis

As for the qualitative evaluation of parameter sensitivity, we found model parameters for characterizing dermal exposure (P_{FO}, D, u_1) were the main contributors to the overall variance of both serum AUC and C_{max} of four targeted BPs (Fig. S3–6). With respect to the cumulative density functions (CDFs) for AUC and C_{max} of unconjugated individual BPs in serum for women, the MC analysis indicated that the adapted PBTK models had medium uncertainty for four targeted BPs (Table 3).

3.4. Model application

We applied the validated models to predict the concentrations of unconjugated BPs in gonads for adult women (18 to 45 years) who were assumed to be dermally exposed to four individual BPs at equal dose every day. As shown in Fig. S7, the lower internal doses in female gonads caused by dermal exposure to BPs via TPs and/or PCPs were predicted by the adapted

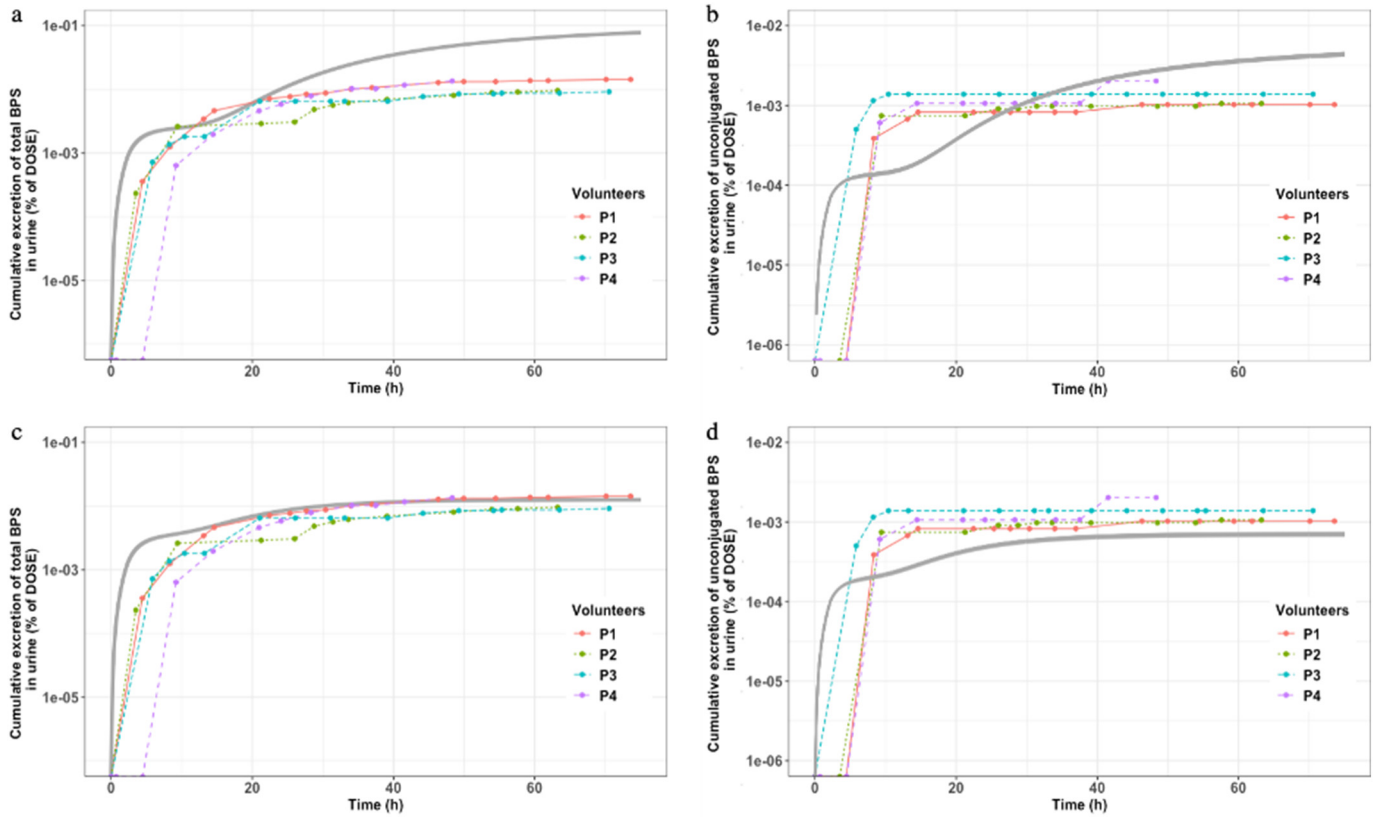

Fig. 4. Visual inspection of measured and simulated urine excretion total and unconjugated amount of BPS-d_8 as a function of time following a dermal exposure to 10 mg/g BPS-d_8 TP. P1–P4 represents 4 volunteers in this study (color circles with color lines). Profiles for the cumulative excretion of BPS-d_8 in urine (grey solid lines) simulated by the adapted dermal PBPK model before calibration (a, b) and after calibration (c, d). Note: BPS, bisphenol S; TP, thermal paper.

PBPK models compared with the previous PBPK models (Karrer et al., 2018). Furthermore, in terms of the internal exposure level of unconjugated BPs in gonads of female adults. BPA exposure via PCPs route resulted in the highest internal exposure followed by BPA exposure via TPs route, BPF exposure via PCPs route, BPAF exposure via PCPs route, and BPS exposure via TPs route (Fig. S8).

4. Discussion

The present study for the first time systematically studied the physiologically based modeling of human dermal absorption of BPA and its high-concerned substitutes including BPS, BPF, and BPAF. A parallel-layered skin compartment model was first proposed for modeling of pharmacokinetics of four BPs in humans following dermal exposure to BPs via TP and PCPs pathways, and integrated into the existing PBPK models for BPs from Karrer et al. (2018). Based on human dermal administration studies, the dermal bio-accessibilities for BPS in TP and for BPF and BPAF in PCPs and urinary pharmacokinetics of BPS were further investigated. The adapted PBPK models for targeted BPs were calibrated, validated and evaluated for prediction of the pharmacokinetic data of BPS and BPA in serum and urine from human studies. The predicted internal dose of BPS, BPF or BPAF to the gonad in a female adult was finally compared with those of BPA.

Table 2
Comparison of observed and predicted pharmacokinetic parameters for BPA in 10 adults following dermal administration of 0.1 mg/kg bw of BPA-d_6 (Sasso et al., 2020).

	Unconjugated BPA-d_6		Total BPA-d_6	
	Observed	Predicted*	Observed	Predicted*
Serum				
C_{max} (nmol/L)	0.27 ± 0.14	0.20	13.26 ± 2.31	11.50
AUC (nmol/L·h)	7.51 ± 2.69	7.33	95.60 ± 54.40	89.90
Urine				
Cumulative excretion (%)	–	–	1.00 ± 0.55	1.31

BPA, bisphenol A; C_{max}: maximum serum concentration; AUC: area under the curve.
* Using the adapted dermal PBPK model for BPA in this study.

The lipophilicity and molecular weight are key determinants of absorption kinetics for BPs in the epidermis. The proposed parallel-layered skin compartment model thus distinguished between the SC and VE of subcompartments. The SC mainly provides the resistance to permeation of highly hydrophilic chemicals and/or high molecular weight, while the relatively hydrophilic VE contributes a significant resistance to permeation of highly lipophilic chemicals. The transient expression in SC is provided by Fick's second law of diffusion in that it describes the non-steady state diffusion of chemicals. The previous studies indicated that the SC is a dynamic barrier as it is continuously formed and shed (i.e. desquamation) over the 1–3 weeks period (Baker and Kligman, 1967), and both BPA and BPS dermal absorption would lead to the prolonged exposure with detectable BPA-d_{16} and BPS in urine for 9 days and 3 days, respectively (Liu and Martin, 2017, 2019). Accordingly, we argued the effect of SC desquamation on skin penetration of chemicals could not be neglected. The quantitative mathematical model studies showed that SC desquamation can significantly reduce subsequent chemical absorption into the systemic circulation for highly lipophilic ($logK_{ow} > 4$) or high molecular weight (MW > about 350 Da) chemicals (Reddy et al., 2000) due to fast epidermal turnover relative to their diffusion through SC. However, BPA and three substitutes in this study are not highly lipophilic or high molecular weight (Table S1). The same SC desquamation velocity u1 by referring to Simon and Goyal (2009) was thus applied to formulate the normal SC desquamation. In addition, the previous in vitro (Champmartin et al., 2020) and in vivo studies (Liu and Martin, 2019) showed that BPA had greater dermal absorption fraction than BPS, which might result from the heavier resistance to BPS than

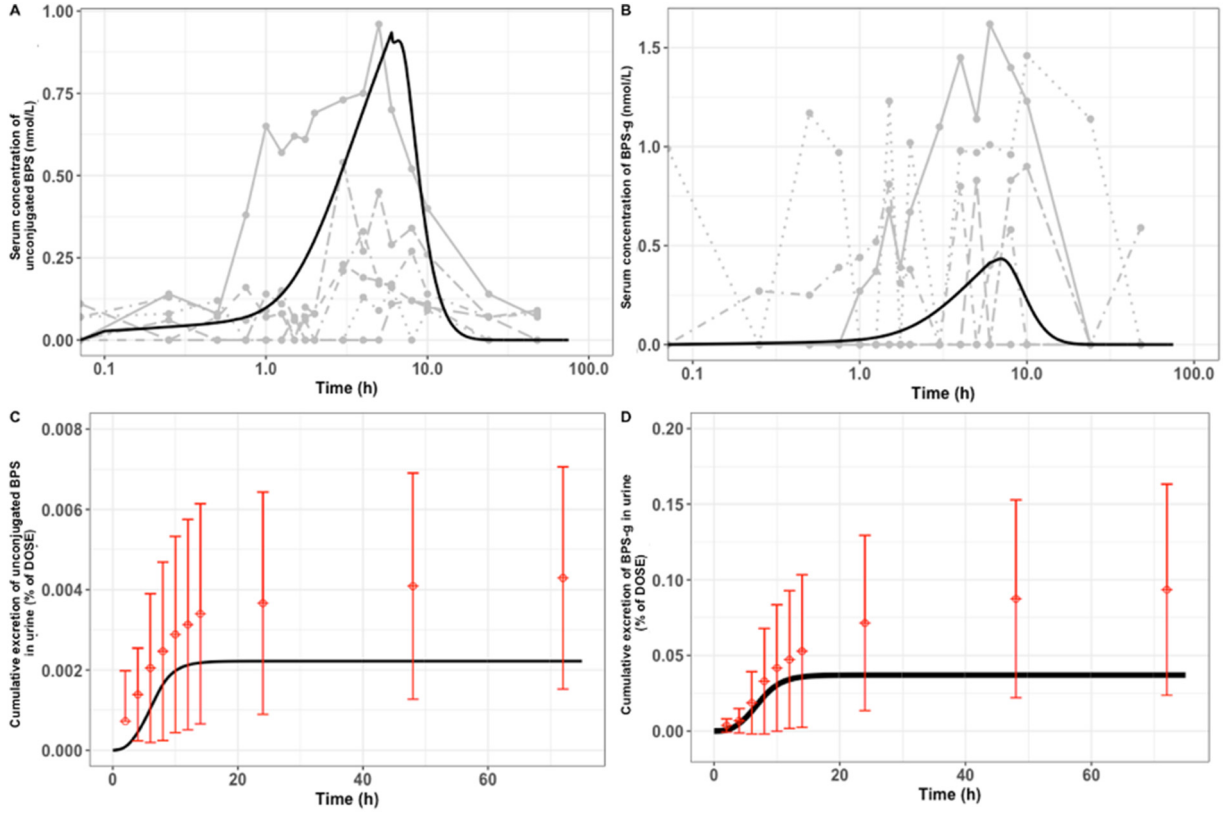

Fig. 5. Observed and predicted serum concentration and urine cumulative excretion amount of unconjugated BPS (A, C) and BPS-g (B, D) after dermal contact with 1 mg/kg bw BPS PCPs (Khmiri et al., 2020). Individual serum measurements (grey circles with grey lines) and urine measurements (red circles with lines) represent the observed (average ± standard deviation) of 6 adults. Profiles for the average volunteers (black solid lines) were modeled by the PBPK model for BPS after calibration. Note: BPS, bisphenol S; BPS-g, BPS glucuronide; PCPs, personal care products; PBPK, physiologically based pharmacokinetic.

BPA in SC since BPS has comparatively lower lipophilicity ($LogK_{ow} \approx 1.29$, https://comptox.epa.gov/dashboard/chemical/details/DTXSID3022409). Nevertheless, during the period of post-exposure the time for the first occurrence of detectable BPS in the receptor in vitro (Champmartin et al., 2020; Liu and Martin, 2019) or in urine of this study is comparable with that of BPA reported by Liu and Martin (2017). We therefore inferred except for the SC and VE pathway for absorption of BPs, there should be potential shunt pathways provided by the follicles and sweat ducts which may also considerably contribute to absorption of BPs soon after application (Otberg et al., 2008). Consequently, the follicle sub-compartment was added into the parallel-layered skin compartment model and its absorption kinetics was characterized by permeability coefficient due to the lack of relevant research. The skin dermis is generally not regarded as a barrier for mass transfer due to the rich vasculature and lymphatic drainage within this layer in vivo that usually has sufficient blood flow to efficiently clear away all chemicals (Roberts et al., 2021).

Table 3
Values for AUC and C_{max} of unconjugated bisphenols in serum predicted for females in Monte Carlo analysis (n = 10,000).

Bisphenols	Mean	SD	5 %	50 %	95 %	Uncertainty coefficient
AUC						
BPA	20.34	6.78	11.19	19.21	33.45	1.74
BPS	1.80	0.60	0.99	1.70	2.86	1.68
BPF	6.30	2.10	3.47	5.95	10.12	1.70
BPAF	0.54	0.18	0.30	0.51	0.87	1.71
C_{max}						
BPA	1.92	0.57	1.13	1.92	2.83	1.47
BPS	0.17	0.05	0.10	0.17	0.23	1.38
BPF	0.60	0.18	0.35	0.60	0.85	1.42
BPAF	0.05	0.02	0.03	0.05	0.07	1.40

Note: AUC: area under the curve; C_{max}: maximum serum concentration; BPA, bisphenol A; BPS, bisphenol S; BPF, bisphenol F; BPAF bisphenol AF; SD, standard deviation.

In the present study human dermal administration studies were conducted to investigate the bio-accessibilities for high-concerned BPA alternatives like BPS, BPF and BPAF. The average dermal bio-accessibility of 26.96 % was obtained for BPS via TP exposure pathway under normal conditions. The variability of dermal bio-accessibility may be associated with different conditioned fingers (e.g. sweaty, very greasy) as well as different types of TP (e.g. cash receipt, ticket). However, Biedermann et al. (2010) reported no significant difference in the amount of BPA transferred from TP to different sites of dry fingers. Furthermore, Eckardt and Simat (2017) also found that no difference in the release of between BPS and BPA were observed from uncoated TP surfaces to "normal" conditioned fingers. Accordingly, the bio-accessibility of BPS (26.96 %) obtained from this study was applied to BPA for the sake of conservative estimation of BPA exposure risk since the low absorption faction for BPA (20 %) in TP[37] was used in previously reported PBPK model for BPA which might underestimate the risk of dermal exposure to BPA in TP. The bio-accessibility of BPA alternatives in PCPs were obtained at 31.65 % for BPF and 12.49 % for BPAF, respectively. They were lower than that for BPA at 60 % (Karrer et al., 2018). These could be explained by the relative lower $LogK_{ow}$ for BPF (2.90, https://comptox.epa.gov/dashboard/chemical/properties/DTXSID9022445) while higher average mass for BPAF (336.2) compared to BPA ($LogK_{ow}$ at 3.50, average mass at 228.3, https://comptox.epa.gov/dashboard/chemical/properties/DTXSID7020182). Zeng et al. (2019) revealed the positive correlation between K_{ow} (<4.90) and dermal bio-accessibility. Besides, as reported in the study of Luo et al. (2020), the dermal bio-accessibility of polycyclic aromatic hydrocarbons (PAHs) was generally correlated with $LogK_{ow}$ and low molecular weight PAHs were much more

easily absorbed via dermal contact than high molecular weight PAHs. Additionally, the obtained dermal bio-accessibility of BPF is in line with the recent in vitro skin absorption test in which 28.2 % of the applied BPF could be absorbed (Lee et al., 2022).

TP contact has been evaluated by the EFSA as the second most important pathway for human exposure to BPA (EFSA, 2015). As one of major substitutes for BPA, BPS pharmacokinetics in humans following dermal exposure via handling TPs was investigated in this study. The proportion of unconjugated BPS-d_8 in urinary total BPS-d_8 was measured to be 11.10 % ± 3.79 % and the occurrence of C_{max} ranged between 14 and 29 h of post-exposure. Similar results were obtained by Liu and Martin (2019) who observed that the proportion of free BPS in total BPS was 6.9 % ± 2.8 % in all urine samples with detectable free BPS and the C_{max} occurred at post-exposure of from 14.2 through 26.4 h for five volunteers; they also found that BPS was not detectable in serum samples collected over 7.5 h and at 22 or 51 h after touching simulated receipts containing BPS. Khmiri et al. (2020) recently reported that plasma levels of BPS and its metabolites in humans were hardly detectable at most time points following skin application to 1 mg/kg bw of BPS-d_8. In this study much less dose of BPS (0.1 mg) was dermally applied which would result in the BPS undetectable in serum, the mere urinary PK data was therefore obtained to implement model calibration and validation. Predictions from the adapted BPA model corresponded well to the measured PK data; otherwise, the adapted model predicted higher serum unconjugated BPS along with lower urine unconjugated BPS and lower BPS-g in serum and urine, which suggested the glucuronidation of BPS in vivo might be underestimated. One possible explanation might be the fact that the adapted BPS model did not consider the metabolism of absorbed BPS in viable human skin. Champmartin et al. (2020) conducted the in vitro experiment using the human skin to access the absorption and metabolism of BPs. They found that the percentage of non-metabolized BPs in the receptor fluid ranged from 84.7 % to 96.1 % after 40 h exposure, indicating that the metabolism of BPs might occur in the skin. Besides, Liu and Martin (2019) discovered the difference between the concentrations of unconjugated BPS and total BPS in the skin tissue and reported >70 % of total BPS was unconjugated in the skin tissue and receiver solutions at 25 h of postdosing, which also demonstrated the existence of glucuronidation of BPS in skin. In addition, Khmiri et al. (2020) reported that the ratio of urinary free BPS-d_8 to total BPS-d_8 was 4.3 % when BPS-d_8 were applied on 40 cm^2 of the forearm in volunteers. But the higher ratio of urinary free BPS-d_8 to total BPS-d_8 (11.10 %) was observed in this study when BPS-d_8 was administered to about 12 cm^2 for 6 finger pads. The results suggested BPS would be metabolized in human skin and BPS metabolism may be related to exposed skin area. After model calibration, the good predictions of internal dose of BPS in serum and urine were obtained by the adapted dermal PBPK models (Figs. 4, 5) rather than the previous PBPK model (Karrer et al., 2018) as shown in Fig. S9, S10. Spontaneous deconjugation of BPs metabolites in biological matrices may also be found in certain conditions. However, the possibility for spontaneous deconjugation of BPS-G in urine samples to unconjugated form is less likely in this study because all urine samples were rapidly collected and stored frozen at −20 °C for limited duration. As shown in Fig. S1c, we found that the predicted amounts for unconjugated BPS in urine using the previous PBPK model (Karrer et al., 2018) were apparently higher than the measured urinary data from the publication of Oh et al. (2018). If the conjugated BPS metabolites in urine samples were spontaneously transferred into the unconjugated form in Oh et al. (2018) study, on the contrary, the discrepancies observed for urinary unconjugated BPS levels between PBPK models output and data from the publication of Oh et al., 2018 should become narrower. Consequently, this effect could have little impact on PBPK models output.

Model uncertainty analysis showed that the adapted dermal PBPK models had medium uncertainty for four targeted BPs. GSA has revealed that these model uncertainties may be mainly attributed to the variabilities of dermal absorption parameters (e.g. P_{FO}, D, u1) and the physiological parameters. These could be explained by the fact that dermal absorption parameters directly affect the uptake amount of BPs which go through the skin and travel into the systemic circulation. The inter-individual difference in the skin status and the site exposed to BPs where the thickness of skin varied could account for the uncertainties of P_{FO}, D and u1. However, the quantification of the variability in distribution for these parameters were currently lacking and CVs at 30 % were therefore assumed for them (Karrer et al., 2018). Overall, the medium uncertainties in the model parameters were reasonable and so the adapted models appear to have the medium reliability.

As for human dermal exposure to BPF and BPAF, the internal dose metrics at adult female gonads predicted by the adapted dermal PBPK models were one order of magnitude or above lower than those predicted by PBPK models from Karrer et al. (2018). The discrepancy between these two predictions could be attributed to the fact that the dermal bioaccessibility of 60 % for BPF and BPAF in the PBPK models from Karrer et al. (2018) were directly derived from that of BPA, which was much large in comparison with those obtained in this study at 31.65 % for BPF and 12.49 % for BPAF, respectively. It obviously would cause the overestimation of internal dose of BPF and BPAF using the previous models. Furthermore, in contrast to the previous PBPK model for BPA in which the single homogeneous well-stirred skin compartment was used, the multiple layered skin compartment model with follicle and other chemical-specific parameters were applied to modeling of percutaneous absorption of BPs in this study. The high skin resistance in SC to the permeation of low lipophilicity of BPS and BPF while great average molecular mass of BPAF may also lead to less dermal absorption of them. In addition, the adapted models predicted a decrease of two orders of magnitude in the internal dose to the female gonads for human exposure to BPS via TP contact compared with BPA (Fig. S7B–C, Fig. S8). Similar results were observed from two in vitro studies. Reale et al. (2021) found only 0.4 % of the applied BPS was recovered in receptor fluid, whereas 25 % of the applied BPA was detected in skin absorption test through ex vivo human skin using flow-through diffusion cells. Liu and Martin (2019) reported that the recoveries of BPS (6.4 %–8.0 %) in receiver solution were smaller than those of 43 %–46 % for BPA, but the used skin thicknesses of 120 μm was thinner than “normal” (verse “moist”) human finger pad with the thickness of 890 to 1300 μm.

This is the first study to investigate physiologically based modeling of human dermal absorption of BPA high-concerned substitutes including BPS, BPF, and BPAF. However, several limitations should be acknowledged and addressed in future studies. Firstly, since there is currently no consistency protocol for human dermal administration study, deviations may occur in these experiments; Secondly, the dermal PBPK models for BPF and BPAF need further validation based on human PK data to improve their reliabilities. Thirdly, in view of the prolonged dermal absorption process for BPs in skin tissue, the metabolism of these chemicals in skin deserves further exploration and consideration. Fourthly, the volunteers wore nitrile gloves on both hands to avoid contagion after dosing in the present study. Due to glove occlusion, the hyperhydration of SC might result in increasing dermal absorption of BPS ($LogK_{ow}$ of 1.29). However, increasing hydration does not always increase skin penetration rates. For example, Bucks et al. (1988) reported that hydration diminished the penetration rate of hydrophilic compounds like hydrocortisone ($LogK_{ow}$ of 1.61). A further research should be performed.

5. Conclusions

In the present study we developed human dermal PBPK models for BPA and three high-concerned substitutes, in which the parallel-layered skin compartment model was for the first time applied to modeling of human dermal exposure to BPs and the dermal bio-accessibilities of BPS in TPs and BPF and BPAF in PCPs were first obtained from human dermal administration studies. Compared with the previous models for BPs, the adapted dermal PBPK models enabled us to more accurately predict the internal dose at target organs following human dermal exposure to BPA and its substitutes via TPs and PCPs routes. This study thus addressed the knowledge gap in physiologically based pharmacokinetic (PBPK) modeling of BPA

and its high-concerned substitutes (BPS, BPF and BPAF) following human dermal exposure.

CRediT authorship contribution statement

Man Hu: Methodology; Investigation; Software; Formal analysis; Visualization; Writing – original draft. Zhichun Zhang: Methodology; Investigation; Writing – revision. Yining Zhang: Methodology; Investigation. Ming Zhan: Methodology. Weidong Qu: Writing – review & editing, Funding acquisition. Gengsheng He: Supervision; Funding acquisition. Ying Zhou: Conceptualization; Methodology; Supervision; Writing – review & editing; Project administration; Funding acquisition.

Data availability

Data will be made available on request.

Declaration of competing interest

The authors declare that they have no known competing financial interests or personal relationships that could have appeared to influence the work reported in this paper.

Acknowledgements

This work was supported by grants from the State Key Program of National Natural Science Foundation of China [81930094], the National Key Research and Development Program of China [2017YFC1600500], the National Natural Science Foundation of China (No. 81373089) and Scientific Research Foundation of Shanghai Pudong New Area Commission of Health and Family Planning (PW2017A-13).

Appendix A. Supplementary data

Supplementary data to this article can be found online at https://doi.org/10.1016/j.scitotenv.2023.161639.

References

Asimakopoulos, A.G., Xue, J., De Carvalho, B.P., Iyer, A., Abualnaja, K.O., Yaghmoor, S.S., Kumosani, T.A., Kannan, K., 2016. Urinary biomarkers of exposure to 57 xenobiotics and its association with oxidative stress in a population in Jeddah,Saudi Arabia. Environ. Res. 150, 573–581. https://doi.org/10.1016/j.envres.2015.11.029.

Baker, H., Kligman, A.M., 1967. Technique for estimating turnover time of human stratum corneum. Arch. Dermatol. 95 (4), 408–411.

Barboza, L.G.A., Cunha, S.C., Monteiro, C., Fernandes, J.O., Guilhermino, L., 2020. Bisphenol a and its analogs in muscle and liver of fish from the North East Atlantic Ocean in relation to microplastic contamination. Exposure and risk to human consumers. J. Hazard. Mater. 393, 122419. https://doi.org/10.1016/j.jhazmat.2020.122419.

Bernier, M.R., Vandenberg, L.N., 2017. Handling of thermal paper: implications for dermal exposure to bisphenol a and its alternatives. PLoS One 12 (6), e0178449. https://doi.org/10.1371/journal.pone.0178449.

Biedermann, S., Tschudin, P., Grob, K., 2010. Transfer of bisphenol A from thermal printer paper to the skin. Anal. Bioanal. Chem. 398 (1), 571–576. https://doi.org/10.1007/s00216-010-3936-9.

Bookout Jr., R.L., Quinn, D.W., McDougal, J.N., 1997. Parallel dermal subcompartments for modeling chemical absorption. SAR QSAR Environ. Res. 7 (1–4), 259–279. https://doi.org/10.1080/10629369708039133.

Buckley, J.P., Kim, H., Wong, E., Rebholz, C.M., 2019. Ultra-processed food consumption and exposure to phthalates and bisphenols in the US National Health and Nutrition Examination Survey, 2013–2014. Environ. Int. 131, 105057. https://doi.org/10.1016/j.envint.2019.105057.

Bucks, D.A., McMaster, J.R., Maibach, H.I., Guy, R.H., 1988. Bioavailability of topically administered steroids: a "mass balance" technique. J. Investig. Dermatol. 91 (1), 29–33. https://doi.org/10.1111/1523-1747.ep12463284.

Chen, L., Li, D., Huang, Y., Zhu, W., Ding, Y., Guo, C., 2020. Preparation of sludge-based hydrochar at different temperatures and adsorption of BPA. Water Sci. Technol. 82 (2), 255–265. https://doi.org/10.2166/wst.2020.096.

Chen, D., Kannan, K., Tan, H., Zheng, Z., Feng, Y.L., Wu, Y., Widelka, M., 2016. Bisphenol analogues other than BPA: environmental occurrence, human exposure, and toxicity. Environ. Sci. Technol. 50 (11), 5438–5453. https://doi.org/10.1021/acs.est.5b05387.

Champmartin, C., Marquet, F., Chedik, L., Décret, M.J., Aubertin, M., Ferrari, E., Grandclaude, M.C., Cosnier, F., 2020. Human in vitro percutaneous absorption of bisphenol S and bisphenol A: a comparative study. Chemosphere 252, 126525. https://doi.org/10.1016/j.chemosphere.126525.

Demierre, A.L., Peter, R., Oberli, A., Bourqui-Pittet, M., 2012. Dermal penetration of bisphenol A in human skin contributes marginally to total exposure. Toxicol. Lett. 213 (3), 305–308. https://doi.org/10.1016/j.toxlet.2012.07.001.

Eckardt, M., Simat, T.J., 2017. Bisphenol A and alternatives in thermal paper receipts - a German market analysis from 2015 to 2017. Chemosphere 186, 1016–1025. https://doi.org/10.1016/j.chemosphere.2017.08.037.

EFSA, 2015. EFSA panel on food contact materials, enzymes, flavourings and processing aids scientific opinion on the risks to public health related to the presence of bisphenol A (bpa) in foodstuffs: executive summary. EFSA J. 13 (1), 3978. https://doi.org/10.2903/j.efsa.2015.3978.

EFSA, 2019. Assessment of the endocrine disrupting properties of Bisphenol AF according to the EU criteria and ECHA/EFSA guidance. EFSA J. 17 (S2), 170914. https://doi.org/10.2903/j.efsa.2019.e170914.

Gajewska, M., Worth, A., Urani, C., Briesen, H., Schramm, K.W., 2014. Application of physiologically-based toxicokinetic modelling in oral-to-dermal extrapolation of threshold doses of cosmetic ingredients. Toxicol. Lett. 227 (3), 189–202. https://doi.org/10.1016/j.toxlet.2014.03.013.

Huang, Y.Q., Wong, C.K., Zheng, J.S., Bouwman, H., Barra, R., Wahlström, B., Neretin, L., Wong, M.H., 2012. Bisphenol a (BPA) in China: a review of sources, environmental levels, and potential human health impacts. Environ. Int. 42, 91–99. https://doi.org/10.1016/j.envint.2011.04.010.

Huang, Z., Zhao, J.L., Yang, Y.Y., Jia, Y.W., Zhang, Q.Q., Chen, C.E., Liu, Y.S., Yang, B., Xie, L., Ying, G.G., 2020. Occurrence, mass loads and risks of bisphenol analogues in the Pearl River Delta region, South China: urban rainfall runoff as a potential source for receiving rivers. Environ. Pollut. 263 (PtB), 114361. https://doi.org/10.1016/j.envpol.2020.114361.

Karrer, C., Roiss, T., von Goetz, N., Gramec Skledar, D., Peterlin Mašič, L., Hungerbühler, K., 2018. Physiologically based pharmacokinetic (PBPK) modeling of the bisphenols BPA, BPS, BPF, and BPAF with new experimental metabolic parameters: comparing the pharmacokinetic behavior of BPA with its substitutes. Environ. Health Perspect. 126 (7), 077002. https://doi.org/10.1289/EHP2739.

Karrer, C., de Boer, W., Delmaar, C., Cai, Y., Crépet, A., Hungerbühler, K., von Goetz, N., 2019. Linking probabilistic exposure and pharmacokinetic modeling to assess the cumulative risk from the bisphenols BPA, BPS, BPF, and BPAF for europeans. Environ. Sci. Technol. 53 (15), 9181–9191. https://doi.org/10.1021/acs.est.9b01749.

Kapraun, D.F., Schlosser, P.M., Nylander-French, L.A., Kim, D., Yost, E.E., Druwe, I.L., 2020. A physiologically based pharmacokinetic model for naphthalene with inhalation and skin routes of exposure. Toxicol. Sci. 177 (2), 377–391. https://doi.org/10.1093/toxsci/kfaa117.

Khmiri, I., Côté, J., Mantha, M., Khemiri, R., Lacroix, M., Gely, C., Toutain, P.L., Picard-Hagen, N., Gayrard, V., Bouchard, M., 2020. Toxicokinetics of bisphenol-S and its glucuronide in plasma and urine following oral and dermal exposure in volunteers for the interpretation of biomonitoring data. Environ. Int. 138, 105644. https://doi.org/10.1016/j.envint.2020.105644.

Krishnan, A.V., Stathis, P., Permuth, S.F., Tokes, L., Feldman, D., 1993. Bisphenol-A: an estrogenic substance is released from polycarbonate flasks during autoclaving. Endocrinology 132 (6), 2279–2286. https://doi.org/10.1210/endo.132.6.8504731.

Lehmler, H.J., Liu, B., Gadogbe, M., Bao, W., 2018. Exposure to bisphenol A, bisphenol F, and bisphenol S in U.S. adults and children: the national health and nutrition examination survey 2013–2014. ACS Omega 3 (6), 6523–6532. https://doi.org/10.1021/acsomega.8b00824.

Lee, S.S., Ryu, H.Y., Ahn, K.S., Lee, S., Lee, J., Lee, J.W., Ko, S.M., Son, W.C., 2022. Toxicological profile of bisphenol F via comprehensive and extensive toxicity evaluations following dermal exposure. J. Toxicol. Environ. Health A 85 (4), 163–174. https://doi.org/10.1080/15287394.2021.1997843.

Liao, C., Liu, F., Alomirah, H., Loi, V.D., Mohd, M.A., Moon, H.B., Nakata, H., Kannan, K., 2012. Bisphenol S in urine from the United States and seven Asian countries: occurrence and human exposures. Environ. Sci. Technol. 46 (12), 6860–6866. https://doi.org/10.1021/es301334j.

Liao, C., Kannan, K., 2014. A survey of alkylphenols, bisphenols, and triclosan in personal care products from China and the United States. Arch. Environ. Contam. Toxicol. 67 (1), 50–59. https://doi.org/10.1007/s00244-014-0016-8.

Liao, C., Kannan, K., 2014. A survey of bisphenol A and other bisphenol analogues in foodstuffs from nine cities in China. Food Addit. Contam. Part A Chem. Anal. Control Expo. Risk Assess. 31 (2), 319–329. https://doi.org/10.1080/19440049.2013.868611.

Li, G., Rabitz, H., Yelvington, P.E., Oluwole, O.O., Bacon, F., Kolb, C.E., Schoendorf, J., 2010. Global sensitivity analysis for systems with independent and/or correlated inputs. J. Phys. Chem. A 114 (19), 6022–6032. https://doi.org/10.1021/jp9096919.

Liu, J., Martin, J.W., 2017. Prolonged exposure to bisphenol A from single dermal contact events. Environ. Sci. Technol. 51 (17), 9940–9949. https://doi.org/10.1021/acs.est.7b03093.

Liu, J., Martin, J.W., 2019. Comparison of bisphenol A and bisphenol S percutaneous absorption and biotransformation. Environ. Health Perspect. 127 (6), 67008. https://doi.org/10.1289/EHP5044.

Liu, B., Lehmler, H.J., Sun, Y., Xu, G., Sun, Q., Snetselaar, L.G., Wallace, R.B., Bao, W., 2019. Associationof bisphenol A and its substitutes, bisphenol F and bisphenol S, with obesity in United States children and adolescents. Diabetes Metab. J. 43 (1), 59–75. https://doi.org/10.4093/dmj.2018.0045.

Lu, S., Yu, Y., Ren, L., Zhang, X., Liu, G., Yu, Y., 2018. Estimation of intake and uptake of bisphenols and triclosan from personal care products by dermal contact. Sci. Total Environ. 621, 1389–1396. https://doi.org/10.1016/j.scitotenv.2017.10.088.

Luo, K., Zeng, D., Kang, Y., Lin, X., Sun, N., Li, C., Zhu, M., Chen, Z., Man, Y.B., Li, H., 2020. Dermal bioaccessibility and absorption of polycyclic aromatic hydrocarbons (PAHs) in indoor dust and its implication in risk assessment. Environ. Pollut. 264, 114829. https://doi.org/10.1016/j.envpol.2020.114829.

Marquet, F., Payan, J.P., Beydon, D., Wathier, L., Grandclaude, M.C., Ferrari, E., 2011. In vivo and ex vivo percutaneous absorption of [14C]-bisphenol A in rats: a possible extrapolation to human absorption? Arch. Toxicol. 85 (9), 1035–1043. https://doi.org/10.1007/s00204-011-0651-z.

OECD, 2007. Series On Testing And Assessment No. 69: guidance document on the validation of (quantitative) structure-activity relationships [(q)sar] models. ENV/JM/MONO(2007)2. http://www.oecd.org/chemicalsafety/risk-assessment/validationofqsarmodels.htm.

Oh, J., Choi, J.W., Ahn, Y.-A., Kim, S., 2018. Pharmacokinetics of bisphenol S in humans after single oral administration. Environ. Int. 112, 127–133. https://doi.org/10.1016/j.envint.2017.11.020.

Otberg, N., Patzelt, A., Rasulev, U., Hagemeister, T., Linscheid, M., Sinkgraven, R., Sterry, W., Lademann, J., 2008. The role of hair follicles in the percutaneous absorption of caffeine. Br. J. Clin. Pharmacol. 65 (4), 488–492. https://doi.org/10.1111/j.1365-2125.2007.03065.x.

Pawar, G., Abdallah, M.A., de Sáa, E.V., Harrad, S., 2017. Dermal bioaccessibility of flame retardants from indoor dust and the influence of topically applied cosmetics. J. Expo. Sci. Environ. Epidemiol. 27 (1), 100–105. https://doi.org/10.1038/jes.2015.84.

Peillex, C., Kerever, A., Lachhab, A., Pelletier, M., 2021. Bisphenol a, bisphenol S and their glucuronidated metabolites modulate glycolysis and functional responses of human neutrophils. Environ. Res. 196, 110336. https://doi.org/10.1016/j.envres.2020.110336.

Poet, T.S., Thrall, K.D., Corley, R.A., Hui, X., Edwards, J.A., Weitz, K.K., Maibach, H.I., Wester, R.C., 2000. Utility of real time breath analysis and physiologically based pharmacokinetic modeling to determine the percutaneous absorption of methyl chloroform in rats and humans. Toxicol. Sci. 54 (1), 42–51. https://doi.org/10.1093/toxsci/54.1.42.

Ranciere, F., Botton, J., Slama, R., Lacroix, M.Z., Debrauwer, L., Charles, M.A., Roussel, R., Balkau, B., Magliano, D.J., D.E.S.I.R. Study Group, 2019. Exposure to Bisphenol A and Bisphenol S and incident type 2 diabetes: a case-cohort study in the French Cohort D.E.S.I.R. Environ. Health Perspect. 127 (10), 107013. https://doi.org/10.1289/EHP5159.

Reale, E., Vernez, D., Hopf, N.B., 2021. Skin absorption of bisphenol A and its alternatives in thermal paper. Ann. Work Expo. Health 65 (2), 206–218. https://doi.org/10.1093/annweh/wxaa095.

Reddy, M.B., Guy, R.H., Bunge, A.L., 2000. Does epidermal turnover reduce percutaneous penetration? Pharm. Res. 17 (11), 1414–1419. https://doi.org/10.1023/a:1007522200422.

Roberts, M.S., Cheruvu, H.S., Mangion, S.E., Alinaghi, A., Benson, H.A.E., Mohammed, Y., Holmes, A., van der Hoek, J., Pastore, M., Grice, J.E., 2021. Topical drug delivery: history, percutaneous absorption, and product development. Adv. Drug Deliv. Rev. 177, 113929. https://doi.org/10.1016/j.addr.2021.113929.

Rochester, J.R., Bolden, A.L., 2015. Bisphenol S and F: a systematic review and comparison of the hormonal activity of bisphenol A substitutes. Environ. Health Perspect. 123 (7), 643–650. https://doi.org/10.1289/ehp.1408989.

Sasso, A.F., Pirow, R., Andra, S.S., Church, R., Nachman, R.M., Linke, S., Kapraun, D.F., Schurman, S.H., Arora, M., Thayer, K.A., Bucher, J.R., Birnbaum, L.S., 2020. Pharmacokinetics of bisphenol A in humans following dermal administration. Environ. Int. 144, 106031. https://doi.org/10.1016/j.envint.2020.106031.

Simon, L., Goyal, A., 2009. Dynamics and control of percutaneous drug absorption in the presence of epidermal turnover. J. Pharm. Sci. 98 (1), 187–204. https://doi.org/10.1002/jps.21408.

Song, S., Ruan, T., Wang, T., Liu, R., Jiang, G., 2012. Distribution and preliminary exposure assessment of bisphenol AF (BPAF) in various environmental matrices around a manufacturing plant in China. Environ Sci Technol. 46 (24), 13136–13143. https://doi.org/10.1021/es303960k.

Toner, F., Allan, G., Dimond, S.S., Waechter Jr., J.M., Beyer, D., 2018. In vitro percutaneous absorption and metabolism of bisphenol A (BPA) through fresh human skin. Toxicol. in Vitro 47, 147–155. https://doi.org/10.1016/j.tiv.2017.11.002.

Von Goetz, N., Pirow, R., Hart, A., Bradley, E., Poças, F., Arcella, D., Lillegard, I.T.L., Simoneau, C., van Engelen, J., Husoy, T., Theobald, A., Leclercq, C., 2017. Including non-dietary sources into an exposure assessment of the European Food Safety Authority: the challenge of multi-sector chemicals such as bisphenol A. Regul. Toxicol. Pharmacol. 85, 70–78. https://doi.org/10.1016/j.yrtph.2017.02.004.

WHO, 2010. Safety, I.P.o.C.; Chemicals, I.-O.P.f.t.S.M.O. Characterization and Application of Physiologically Based Phamacokinetic Models in Risk Assessment. World Health Organization.

Xue, J., Wu, Q., Sakthivel, S., Pavithran, P.V., Vasukutty, J.R., Kannan, K., 2015. Urinary levels of endocrine-disrupting chemicals, including bisphenols, bisphenol A diglycidyl ethers, benzophenones, parabens, and triclosan in obese and non-obese Indian children. Environ. Res. 137, 120–128. https://doi.org/10.1016/j.envres.2014.12.007.

Yang, Y., Guan, J., Yin, J., Shao, B., Li, H., 2014. Urinary levels of bisphenol analogues in residents living near a manufacturing plant in south China. Chemosphere 112, 481–486. https://doi.org/10.1016/j.chemosphere.2014.05.004.

Yang, Y., Yang, Y., Zhang, J., Shao, B., Yin, J., 2019. Assessment of bisphenol A alternatives in paper products from the Chinese market and their dermal exposure in the general population. Environ. Pollut. 244, 238–246. https://doi.org/10.1016/j.envpol.2018.10.049.

Zalko, D., Jacques, C., Duplan, H., Bruel, S., Perdu, E., 2011. Viable skin efficiently absorbs and metabolizes bisphenol A. Chemosphere 82 (3), 424–430. https://doi.org/10.1016/j.chemosphere.2010.09.058.

Zeng, D., Kang, Y., Chen, J., Li, A., Chen, W., Li, Z., He, L., Zhang, Q., Luo, J., Zeng, L., 2019. Dermal bioaccessibility of plasticizers in indoor dust and clothing. Sci. Total Environ. 672, 798–805. https://doi.org/10.1016/j.scitotenv.2019.04.028.

Zhang, H., Quan, Q., Zhang, M., Zhang, N., Zhang, W., Zhan, M., Xu, W., Lu, L., Fan, J., Wang, Q., 2020. Occurrence of bisphenol A and its alternatives in paired urine and indoor dust from Chinese university students: implications for human exposure. Chemosphere 247, 125987. https://doi.org/10.1016/j.chemosphere.2020.125987.